Molecular Therapy
Nucleic Acids
Original Article

Hexose Potentiates Peptide-Conjugated Morpholino Oligomer Efficacy in Cardiac Muscles of Dystrophic Mice in an Age-Dependent Manner

Gang Han,[1,3] Ben Gu,[1,3] Caorui Lin,[1] Hanhan Ning,[1] Jun Song,[1] Xianjun Gao,[1] Hong M. Moulton,[2] and HaiFang Yin[1]

[1]School of Medical Laboratory and Department of Cell Biology, Tianjin Medical University, Tianjin 300070, China; [2]Biomedical Sciences, College of Veterinary Medicine, Oregon State University, Corvallis, OR, USA

Insufficient delivery of oligonucleotides to muscle and heart remains a barrier for clinical implementation of antisense oligonucleotide (AO)-mediated exon-skipping therapeutics in Duchenne muscular dystrophy (DMD), a lethal monogenic disorder caused by frame-disrupting mutations in the *DMD* gene. We previously demonstrated that hexose, particularly an equal mix of glucose:fructose (GF), significantly enhanced oligonucleotide delivery and exon-skipping activity in peripheral muscles of *mdx* mice; however, its efficacy in the heart remains limited. Here we show that co-administration of GF with peptide-conjugated phosphorodiamidate morpholino oligomer (PPMO, namely, BMSP-PMO) induced an approximately 2-fold higher level of dystrophin expression in cardiac muscles of adult *mdx* mice compared to BMSP-PMO in saline at a single injection of 20 mg/kg, resulting in evident phenotypic improvement in dystrophic *mdx* hearts without any detectable toxicity. Dystrophin expression in peripheral muscles also increased. However, GF failed to potentiate BMSP-PMO efficiency in aged *mdx* mice. These findings demonstrate that GF is applicable to both PMO and PPMO. Furthermore, GF potentiates oligonucleotide activity in *mdx* mice in an age-dependent manner, and, thus, it has important implications for its clinical deployment for the treatment of DMD and other muscular disorders.

INTRODUCTION

Duchenne muscular dystrophy (DMD) remains an incurable monogenic disorder, caused by frame-disrupting mutations in the *DMD* gene, resulting in pre-termination of the functional dystrophin protein.[1] Although the approval of the first antisense oligonucleotide (AO) drug (eteplirsen), which functions by removing mutated exons and restoring reading frame of the *DMD* gene, brought hope and excitement for the DMD community, its efficacy needs to be improved for clinical deployment, as only negligible levels of functional dystrophin protein were detected in treated DMD patients.[2,3] Despite recent studies demonstrating that the sequence selection might not be optimal,[4] insufficient delivery of AOs largely accounts for its inefficiency.

A myriad of strategies to enhance the systemic delivery efficiency of AOs has been under scrutiny, including the use of cell-penetrating peptides (CPPs), nanoparticles, viruses, and small compounds.[5,6] Among them, CPPs led the way due to advantages such as small molecular weight and high membrane permeabilization capacity; however, the safety profiles present a hurdle for their clinical translation.[7] Nanoparticles including synthetic and natural biological nanoscale vesicles such as exosomes have been explored as delivery vehicles for AOs, wherein the former showed limited efficacy and the latter is still in early development.[6,8] Recently, small compounds have found favor, particularly the ones used in the clinic for other therapeutic purposes, such as dantrolene and hexose, which showed promise as adjuvants to enhance AOs' efficacy and can be fast-tracked to the clinic.[9–12]

We previously demonstrated that hexose, particularly the mixture of 2.5% glucose and 2.5% fructose (GF), could augment the activity of phosphorodiamidate morpholino oligomers (PMOs) in peripheral muscles and elicit long-term beneficial effect on *mdx* mice.[11,12] However, most DMD patients suffer from cardiac failure, which is the leading cause for the mortality of DMD patients.[13] Here we evaluated the potency of GF to enhance the activity of AOs in cardiac muscles of dystrophic mice with a chimeric peptide-conjugated PMO (namely, BMSP-PMO), which was shown to be efficacious in both peripheral and cardiac muscles of adult *mdx* mice.[14] We demonstrated that GF augmented the activities of BMSP-PMO in peripheral, smooth, and cardiac muscles of adult *mdx* mice but failed in aged *mdx* mice, indicating that GF functions in an age-dependent manner. Therefore, our study unveils the functionality of GF in enhancing the potency of AOs in dystrophic hearts, and it also provides evidence for the potentially applicable DMD populations.

RESULTS

GF Augments Peptide-Conjugated PMO Activities in Peripheral Muscles of Adult *mdx* Mice

To assess the capacity of GF to potentiate the activity of peptide-conjugated PMOs, we co-administered GF with BMSP-PMO

Received 2 August 2019; accepted 14 September 2019;
https://doi.org/10.1016/j.omtn.2019.09.012.

[3]These authors contributed equally to this work.

Correspondence: HaiFang Yin, PhD, Department of Cell Biology, Tianjin Medical University, Qixiangtai Road, Heping District, Tianjin 300070, China.
E-mail: haifangyin@tmu.edu.cn

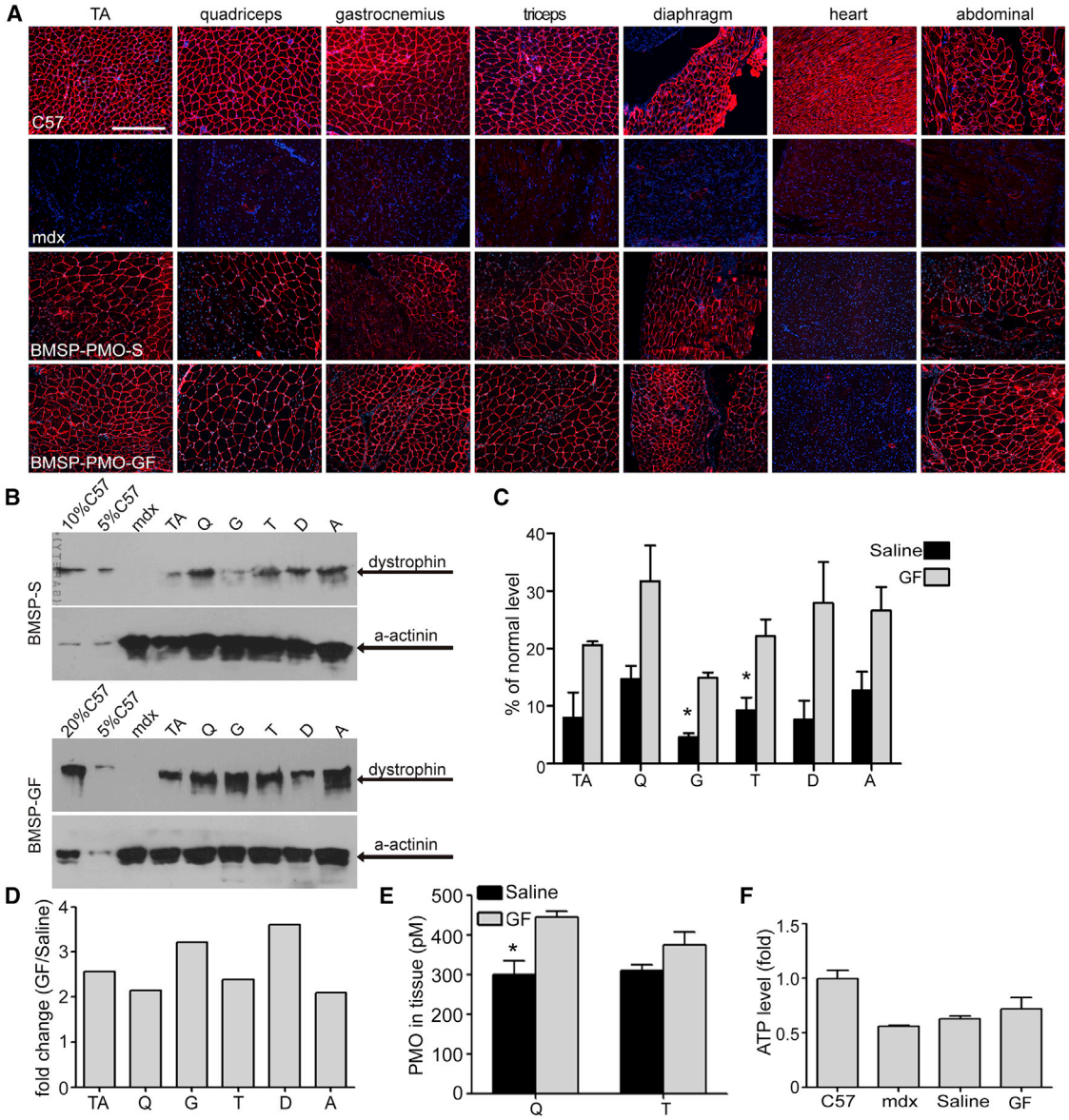

Figure 1. Dystrophin Restoration in Adult *mdx* Mice Treated with a Single Intravenous Injection of 6 mg/kg BMSP-PMO-GF or BMSP-PMO-S

(A) Immunohistochemistry for dystrophin expression in body-wide muscles from adult *mdx* mice treated with BMSP-PMO-GF or BMSP-PMO-S (scale bar, 100 μm). (B) Representative western blot image to show dystrophin restoration in *mdx* mice treated with BMSP-PMO-GF. 2.5, 5, and 10 μg total protein from *C57BL6* and 50 μg from untreated and treated *mdx* muscle samples were loaded, respectively. α-actinin was used as the loading control. (C) Quantitative analysis of western blot results with ImageJ (*$p < 0.05$). TA, tibialis anterior; Q, quadriceps; G, gastrocnemius; T, triceps; D, diaphragm; A, abdominal muscle. The data are presented as mean ± SEM unless otherwise specified (n = 3). Saline and GF refer to BMSP-PMO-S or BMSP-PMO-GF, respectively. (D) Fold change for BMSP-PMO-GF relative to BMSP-PMO-S. (E) Quantification of PMO levels in quadriceps and triceps from treated *mdx* mice with ELISA (n = 3, *$p < 0.05$). (F) Measurement of ATP levels in quadriceps of treated adult *mdx* mice (n = 3). Significance was determined with a two-tailed t test.

(BMSP-PMO-GF) at the dose of 6 mg/kg as a single intravenous injection in adult *mdx* mice, as this dose was shown to be effective in peripheral muscles.[14] We reasoned that a low but effective dose of BMSP-PMO would allow differentiating GF's enhancement on BMSP-PMO activities. As expected, BMSP-PMO-GF induced more dystrophin-positive fibers and significantly higher levels of dystrophin restoration than BMSP-PMO in saline (BMSP-PMO-S) in skeletal muscles of treated *mdx* mice, though no dystrophin was found in the heart at this dose (Figures 1A–1C). Up to a 3.6-fold higher level of dystrophin protein was detected in the diaphragm of BMSP-PMO-GF-treated *mdx* mice compared to BMSP-PMO-S (Figure 1D).

Likewise, GF also enhanced the activity of R-PMO, another peptide-conjugated PMO shown to be effective in *mdx* mice,[15] in peripheral muscles of treated adult *mdx* mice, as dystrophin-positive fibers and levels of dystrophin protein dramatically increased in most peripheral muscles from mice treated with R-PMO in GF compared to the saline group under identical conditions (Figures S1A–S1C).

To verify if the enhanced activity was due to an increased uptake of PMO, we measured PMO in peripheral muscles. Consistent with previous observations,[11] the amount of PMO was significantly elevated in quadriceps of BMSP-PMO-GF-treated *mdx* mice compared to corresponding tissues from BMSP-PMO-S-treated *mdx* mice (Figure 1E). However, the ATP level in the quadriceps of BMSP-PMO-GF-treated *mdx* mice only marginally rose compared to BMSP-PMO-S (Figure 1F), suggesting that a small increase in ATP levels likely enables amplified effect on the uptake of BMSP-PMO, resulting in enhanced activities. These results demonstrate that GF can augment the efficacy of cell-penetrating peptide-PMO conjugates by improving cellular uptake, which is presumably taken up by a separate pathway from unmodified PMO.[11,16–19]

GF Fails to Enhance BMSP-PMO Activities in Aged *mdx* Mice

Given 6 mg/kg BMSP-PMO-GF was unable to induce dystrophin expression in the dystrophic heart, a higher but non-saturating dose of 20 mg/kg might be required to demonstrate GF-induced enhancement of BMSP-PMO activity in *mdx* mice. As aged *mdx* mice were shown to better mimic cardiac abnormalities manifested in DMD patients,[20–22] GF's effects on BMSP-PMO in dystrophic hearts were evaluated in 14-month-old *mdx* mice. Strikingly, a single intravenous injection of BMSP-PMO-GF at the dose of 20 mg/kg elicited substantial numbers of dystrophin-positive fibers in aged *mdx* hearts (Figure 2A), with approximately 30% of normal level of dystrophin protein restored (Figure 2B), though there was no evident difference between the GF and saline groups. Consistently, cardiac function marginally improved as ejection fraction (EF) and fractional shortening (FS) of left ventricles substantially rose and interventricular septum (IVS) thickness and left ventricle mass decreased in BMSP-PMO-treated aged *mdx* mice compared to untreated age-matched *mdx* controls (Figure 2C), though no difference was observed between the GF and saline groups, suggesting that BMSP-PMO is effective in the dystrophic heart but GF failed to augment its activity in aged *mdx* hearts.

Corroborating with the improved heart function, a significant reduction in serum creatine kinase-MB (CK-MB) (Figure 2D), an enzyme found primarily in cardiac muscle cells,[23,24] and decreased fibrotic areas (Figure 2E) and much fewer inflammatory cells (Figure 2F) were seen in BMSP-PMO-treated aged *mdx* hearts compared to untreated age-matched *mdx* controls, with the GF and saline groups showing comparable efficacy. Similar amounts of PMO (Figure 2G) and comparable levels of ATP (Figure 2H) were detected in aged *mdx* hearts treated with BMSP-PMO-GF or BMSP-PMO-S. This implies that GF could not enhance BMSP-PMO activities in aged *mdx* hearts, which seem to be limited in the ability to generate ATP compared to adult *mdx* mice (Figure S2A). Corroborating with the heart data, pronounced and comparable levels of dystrophin expression were present in peripheral muscles of aged *mdx* mice treated with BMSP-PMO-GF or BMSP-PMO-S (Figures S2B–S2D). Similarly, no difference was detected in PMO uptake or ATP levels in peripheral muscles of aged *mdx* mice treated with BMSP-PMO-GF or BMSP-PMO-S (Figures S2E and S2F). These findings indicate that BMSP-PMO is able to rescue the functional impairments in aged *mdx* hearts but GF failed to potentiate its efficacy.

GF Potentiates BMSP-PMO Efficacy in Adult *mdx* Mice

To determine whether GF potentiates BMSP-PMO efficacy in adult dystrophic hearts, we administered BMSP-PMO-GF in adult *mdx* mice under an identical dosing regimen to aged *mdx* mice (20 mg/kg for a single intravenous injection). Strikingly, substantial increases in dystrophin-positive fibers (Figure 3A) and approximately 2-fold higher levels of dystrophin were found in BMSP-PMO-GF-treated adult *mdx* hearts (60% ± 5.9%) compared to BMSP-PMO-S (31% ± 2.0%) (Figure 3B). Concordantly, a significant increase in PMO levels was detected in BMSP-PMO-GF-treated *mdx* hearts compared to BMSP-PMO-S (Figure 3C), though only a marginal increase in the level of ATP was observed (Figure 3D), supporting the notion that GF potentiates BMSP-PMO efficacy in *mdx* hearts by increasing its cellular uptake.

Although the level of dystrophin significantly increased in adult *mdx* hearts, no functional difference was found in treated adult *mdx* hearts compared to age-matched normal and untreated *mdx* controls (Figure S3), as no cardiac abnormality was noticed in adult *mdx* mice employed in the study. Unsurprisingly, near normal myoarchitecture was restored with all skeletal muscle fibers stained positive for dystrophin (Figure S4A), and almost total exon skipping of the mutated transcript was induced (Figure S4B) in adult *mdx* mice treated with BMSP-PMO-GF or BMSP-PMO-S. Levels of dystrophin protein significantly rose in quadriceps and triceps of BMSP-PMO-GF-treated adult *mdx* mice compared to BMSP-PMO-S (Figures S4C and S4D), further confirming the enhancement of GF on BMSP-PMO in peripheral muscles. Corroborating with the low-dose BMSP-PMO data, marginally increased levels of PMO and ATP were detected in the quadriceps of BMSP-PMO-GF-treated *mdx* mice compared to BMSP-PMO-S (Figures S4E and S4F). These results support the conclusion that GF augments BMSP-PMO activity in *mdx* mice in an age-dependent manner.

BMSP-PMO-GF Elicits Phenotypic Improvement in Adult *mdx* Hearts

Given the high activity of BMSP-PMO-GF observed in adult *mdx* hearts, we next examined its ability to restore function and correct disease pathologies in *mdx* mice. Dystrophin-associated protein complex (DAPC) destabilizes and mis-localizes in the absence of dystrophin, and thus the relocalization of DAPC was used as a parameter for functional improvement in DMD patients.[1] Immunohistochemical staining of DAPC components, including β-dystroglycan and α- and β-sarcoglycan, in BMSP-PMO-treated adult

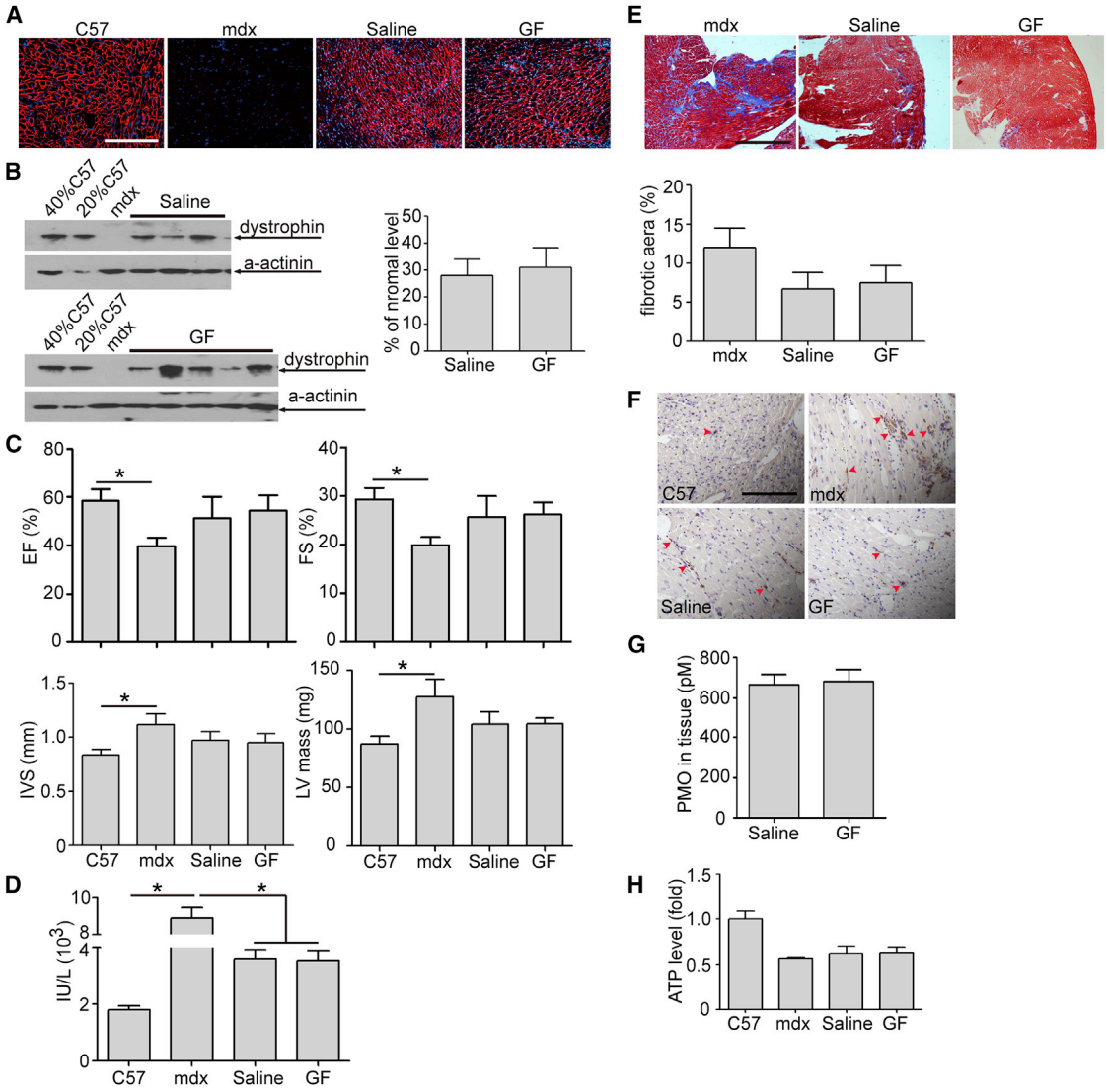

Figure 2. Systemic Evaluation of BMSP-PMO-GF or BMSP-PMO-S in Cardiac Muscles of Aged *mdx* Mice

14-month-old *mdx* mice were treated with BMSP-PMO-GF or BMSP-PMO-S at the dose of 20 mg/kg for a single intravenous injection. (A) Immunohistochemistry for dystrophin expression in the heart from aged *mdx* mice treated with BMSP-PMO-GF or BMSP-PMO-S (scale bar, 50 μm). (B) Representative western blot and quantitative analysis to show dystrophin restoration in aged *mdx* mice treated with BMSP-PMO-GF (n = 5) or BMSP-PMO-S (n = 3). 4 and 8 μg total protein from *C57BL6* and 20 μg from untreated and treated *mdx* muscle samples were loaded, respectively. α-actinin was used as the loading control. (C) Measurement with echocardiography of heart functions in aged *mdx* mice treated with BMSP-PMO-GF (n = 5) or BMSP-PMO-S (n = 4), age-matched *C57BL6* mice (n = 6), and untreated *mdx* controls (n = 8) (*$p < 0.05$). EF and FS refer to ejection fraction and fractional shortening, respectively. IVS means interventricular septum. (D) Measurement of serum creatine kinase-MB (CK-MB) levels in treated aged *mdx* mice (n = 3, *$p < 0.05$). (E) Collagen deposition analysis in hearts from treated aged *mdx* mice (scale bar, 100 μm). (F) Immunohistochemical staining for $CD68^+$ macrophages in hearts from treated aged *mdx* mice (scale bar, 100 μm). Arrowheads point to CD68-positive macrophages. (G) Quantification of PMO levels in heart tissues from treated aged *mdx* mice with ELISA (n = 3). (H) Measurement of ATP levels in hearts of treated aged *mdx* mice (n = 3). Significance was determined with a two-tailed t test.

mdx hearts indicated correct localization in sarcolemmal membrane (Figure 4A). Serum CK-MB levels (Figure 4B) and immunoglobulin (Ig) staining (Figures 4C and 4D) were significantly reduced in BMSP-PMO-GF-treated adult *mdx* hearts compared to BMSP-PMO-S and untreated age-matched *mdx* controls. It indicates the improved membrane integrity of treated *mdx* hearts. A pronounced reduction in collagen deposition/fibrotic areas (Figures 4E and 4F) and much fewer inflammatory cells (Figure 4G) were seen in BMSP-PMO-GF-treated aged *mdx* hearts compared to BMSP-PMO-S and untreated age-matched *mdx* controls, further supporting the conclusion that BMSP-PMO-GF elicits phenotypic improvements in adult *mdx* hearts. These data demonstrate that

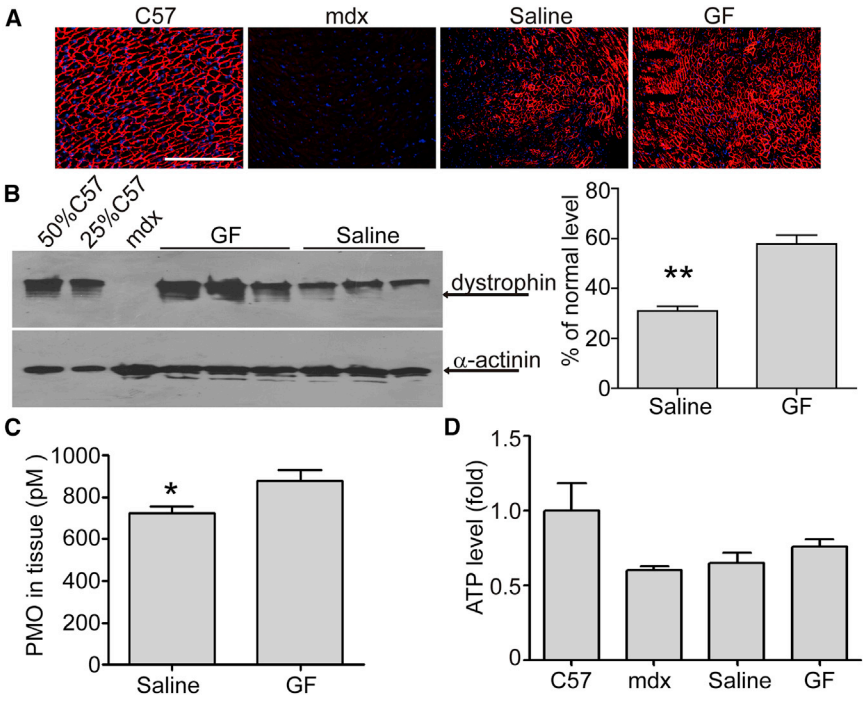

Figure 3. Dystrophin Restoration in Cardiac Muscles of Adult *mdx* Mice Treated with a Single Intravenous Injection of BMSP-PMO-GF or BMSP-PMO-S at 20 mg/kg

(A) Immunohistochemistry for dystrophin expression in the heart from adult *mdx* mice treated with BMSP-PMO-GF (scale bar, 50 μm). (B) Representative western blot and quantitative analysis to show dystrophin restoration in adult *mdx* mice treated with BMSP-PMO-GF or BMSP-PMO-S (n = 3, **p < 0.01). 5 and 10 μg total protein from *C57BL6* and 20 μg from untreated and treated *mdx* muscle samples were loaded, respectively. α-actinin was used as the loading control. (C) Quantification of PMO levels in heart tissues of treated adult *mdx* mice with ELISA (n = 3, *p < 0.05). (D) Measurement of ATP levels in hearts of treated adult *mdx* mice (n = 3). Significance was determined with a two-tailed t test.

BMSP-PMO-GF can elicit molecular correction and phenotypic rescue of adult *mdx* hearts.

Consistent with molecular correction, BMSP-PMO-GF induced phenotypic rescue in peripheral muscles of adult *mdx* mice reflected by significantly increased grip strength (Figure 5A), reduced levels of serum CK (Figure 5B) and decreased numbers of inflammatory cells (Figure 5C), and correct re-localization of DAPC (Figure 5D) in BMSP-PMO-treated adult *mdx* mice compared to untreated age-matched *mdx* controls, though no significant difference was observed between BMSP-PMO-GF and BMSP-PMO-S, which can probably be attributed to high levels of dystrophin expression restored in peripheral muscles.

BMSP-PMO-GF Does Not Evoke Any Overt Toxicity in Adult *mdx* Mice

To determine whether the combination of GF and BMSP-PMO would evoke any toxicity in adult *mdx* mice, we measured serum indices for liver and kidney functions, including γ-Glutamyl Transferase (GGT), aspartate aminotransferase (AST), and alanine aminotransferase (ALT), which are usually elevated in *mdx* mice,[25,26] and creatinine (Cr) and urea (UA). Serum AST and ALT levels significantly declined (Figure 6A) and there was no change in creatinine and urea (Figure 6B) in BMSP-PMO-GF-treated adult *mdx* mice compared to untreated age-matched *mdx* controls, indicating no liver and kidney toxicities. Examination on serum glucose revealed no abnormal increase in BMSP-PMO-GF-treated adult *mdx* mice compared to untreated *mdx* and normal controls (Figure 6C). Consistently, no detectable morphological deformation was found in liver and kidney from *mdx* mice treated with BMSP-PMO-GF, as demonstrated by H&E staining (Figure 6D), showing that BMSP-PMO-GF does not elicit any overt toxicity in *mdx* mice.

DISCUSSION

Enhancing AO activities in the heart remains a hurdle for exon-skipping therapeutics in DMD. Here we investigated the potency of GF on enhancing AO activities in dystrophic hearts by co-administering GF with BMSP-PMO in *mdx* mice. GF significantly enhanced the uptake and activity of BMSP-PMO and elicited phenotypic rescue in peripheral muscle and heart of adult *mdx* mice, but it failed to do so in aged *mdx* mice, indicating an age-related diminution effect. Our data demonstrate that BMSP-PMO is potent in membrane permeabilization and internalization independent of age whereas GF functions in an age-dependent manner. Given GF-based infusions have been extensively employed in clinical practice, this approach can be fast-tracked to the clinic by simply buffering approved AOs with GF. Thus our study provides a general and simple strategy to augment the potency of oligonucleotides and ease the economic burden of DMD patients by reducing the drug-related costs.

With low doses of BMSP-PMO and R-PMO, we were able to show the enhancement of GF on PMO activities but failed to induce any dystrophin expression in the heart, suggesting that a threshold concentration exists for peptide-conjugated PMO. This was verified with the high-dose study, which showed differentiable effect conferred by GF both in cardiac and peripheral muscles of adult *mdx* mice. Notably, due to the high dose employed, the difference between GF and saline in peripheral muscles was less evident, as BMSP-PMO is extremely potent in inducing exon-skipping in *mdx* mice. However, GF was unable to potentiate the activity of BMSP-PMO in aged *mdx* mice, which is likely attributed to the impaired mitochondria as they worsen in aged mice.[27,28]

Notably, the level of dystrophin required for therapeutic improvements in dystrophic hearts remains undetermined, with reports showing a

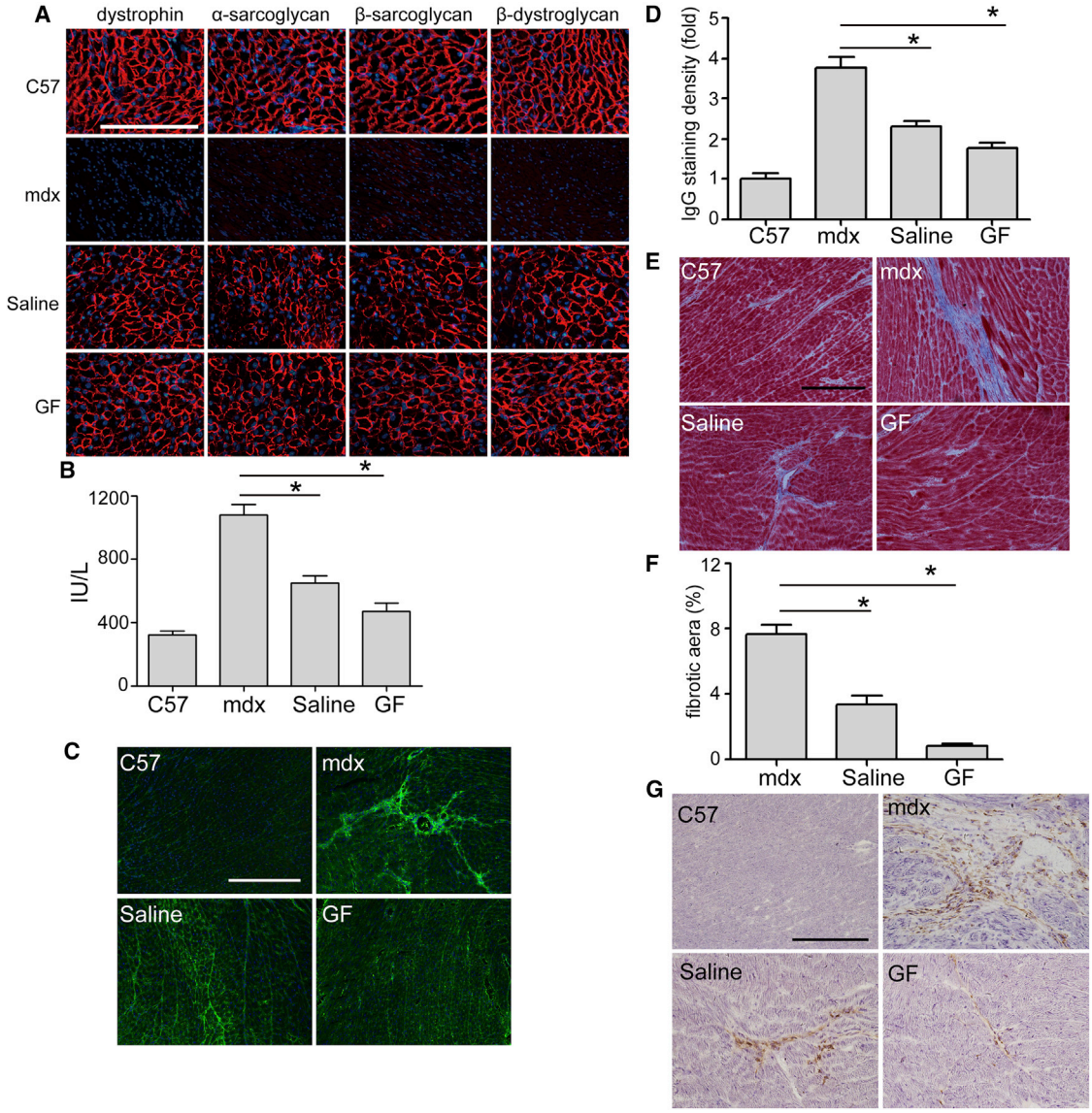

Figure 4. Functional Correction of Cardiac Muscles in Adult *mdx* Mice Treated with a Single Intravenous Injection of BMSP-PMO-GF or BMSP-PMO-S at 20 mg/kg

(A) Re-localization of dystrophin-associated protein complex (DAPC) components in treated dystrophic hearts to assess dystrophin function and recovery of normal myoarchitecture (scale bar, 100 μm). (B) Measurement of serum CK-MB levels in treated adult *mdx* mice (n = 3, *p < 0.05). IgG staining (C) and quantitative analysis (D) to assess the membrane integrity in hearts from adult *mdx* mice treated with BMSP-PMO-GF or BMSP-PMO-S (scale bar, 100 μm) (n = 3, *p < 0.05). Collagen deposition staining (E) and quantitative analysis (F) in hearts from adult *mdx* mice treated with BMSP-PMO-GF or BMSP-PMO-S (scale bar, 100 μm) (n = 3, *p < 0.05). (G) Immunohistochemical staining for $CD68^+$ macrophages in hearts from treated aged *mdx* mice (scale bar, 100 μm). Significance was determined with a two-tailed t test.

range of negligible to near normal levels of dystrophin in hearts in different model systems.[29–32] In our current study, although about 30% of normal level of dystrophin protein was restored in aged dystrophic hearts, there was no significant functional improvement observed in *mdx* mice treated with BMSP-PMO either in saline or GF compared to age-matched *mdx* controls. Interestingly, a significant cardiac improvement was detected in BMSP-PMO-treated aged *mdx* mice when the saline and GF groups were combined (data not shown), suggesting that a large number of aged *mdx* mice are required. Nevertheless, there was no difference between BMSP-PMO in saline and GF. As adult *mdx* mice showed mild cardiac dysfunction, we were unable to demonstrate cardiac functional improvement conferred by GF, though phenotypic and molecular corrections were achieved. Therefore, utrophin and dystrophin double-knockout (DKO) mice will be an ideal model system to evaluate the potency of GF in hearts,[33] and future studies in DKO mice are warranted.

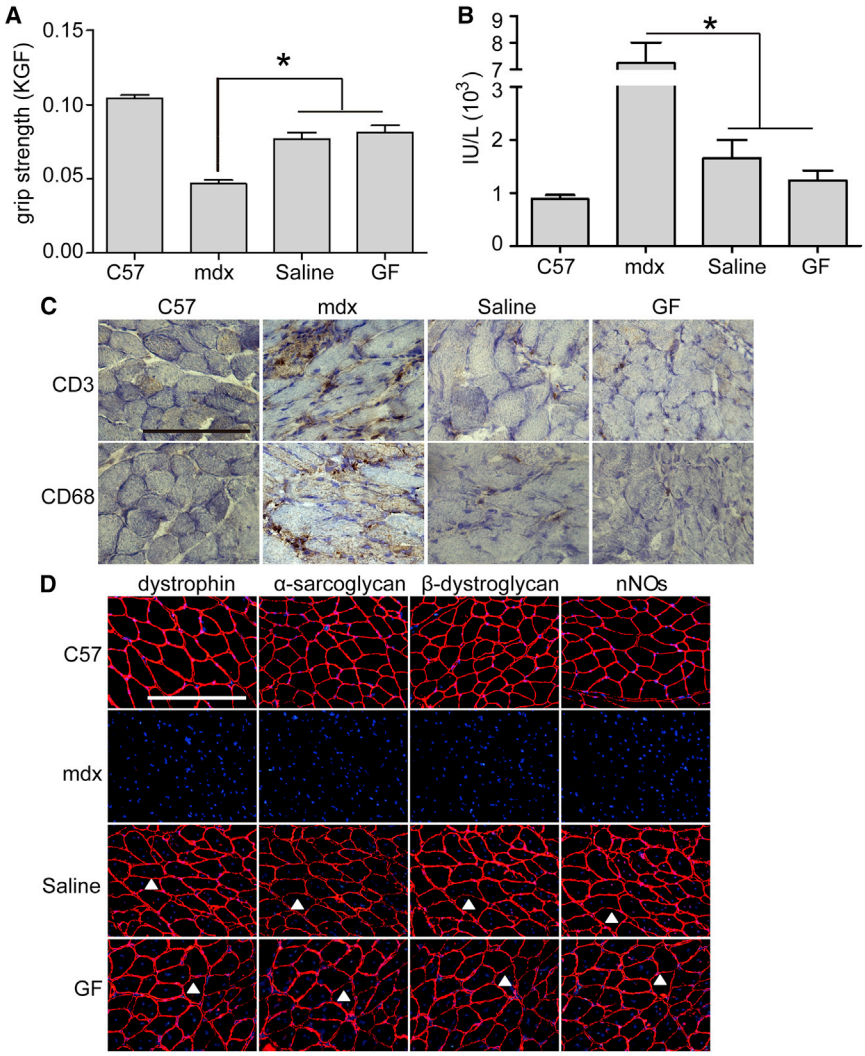

Figure 5. Functional Rescue of Peripheral Muscles in Adult *mdx* Mice Treated with a Single Intravenous Injection of BMSP-PMO-GF or BMSP-PMO-S at 20 mg/kg

(A) Muscle function was assessed with grip strength to determine the physical improvement in adult *mdx* mice treated with BMSP-PMO-GF (n = 6) or BMSP-PMO-S (n = 3, *p < 0.05). (B) Measurement of serum CK levels in treated adult *mdx* mice (n = 3, *p < 0.05). (C) Immunohistochemical staining for $CD68^+$ macrophages in quadriceps from treated adult *mdx* mice (scale bar, 50 μm). (D) Relocalization of DAPC components in quadriceps from treated adult *mdx* mice (scale bar, 100 μm). Significance was determined with a two-tailed t test.

Although GF failed to enhance BMSP-PMO activities in aged *mdx* mice, considering the current trials for exon-skipping therapeutics focus on children and young adults, GF might present a great clinical potential in combination with approved AO drugs for DMD treatment. BMSP-PMO was effective in inducing dystrophin expression in cardiac and peripheral muscles of *mdx* mice independent of ages, further confirming the strong membrane permeability of BMSP.[14] In addition, our previous studies demonstrated that both BMSP-PMO and PMO used the energy-dependent endocytosis pathway,[11,18] and here we showed that GF enables the enhancement of different cargoes utilizing energy-dependent pathways in dystrophic muscles. Notably, although the ATP level was only marginally elevated, GF was able to enhance the uptake of BMSP-PMO in peripheral and cardiac muscles of *mdx* mice, suggesting that a small increase in the level of ATP can generate an amplified effect on PMO uptake. However, we cannot exclude the possibility that other mechanisms might be involved. Strikingly, a significant enhancement was found in smooth muscle such as trachea from BMSP-PMO-GF-treated adult *mdx* mice compared to BMSP-PMO-S at 20 mg/kg (Figures S5A–S5C), suggesting that GF is potent in smooth muscles of *mdx* mice. This is also, to our knowledge, the first report showing the restoration of dystrophin in the trachea of *mdx* mice.

In conclusion, we demonstrate that GF can augment BMSP-PMO activities in cardiac, peripheral, and smooth muscles of *mdx* mice in an age-dependent manner, and thus we provide evidence for the clinical deployment of GF in DMD patient populations. The findings presented here also provide a tool for facilitating the delivery of AOs to cardiac and smooth muscles in DMD and other muscle-related disorders.

MATERIALS AND METHODS

Animals and Injections

Adult *mdx* (6- to 8-week-old) mice, aged *mdx* (14-month-old) mice, and age-matched *C57BL6* mice were used in all experiments (purchased from The Jackson Laboratory, USA; the number for each group is specified in the figure legends). The experiments were carried out in the Animal unit, Tianjin Medical University (Tianjin, China), according to procedures authorized by the institutional ethical committee (permit SYXK 2009-0001). For systemic studies, various amounts of BMSP-PMO or R-PMO in 120 μL saline or GF (2.5% glucose:2.5% fructose) (Sigma, USA) were injected into the tail vein of *mdx* mice at final doses of 6 or 20 mg/kg, respectively. Mice were sacrificed by CO_2 inhalation at 2 weeks after the last injection, muscles and other tissues were snap-frozen in liquid nitrogen-cooled isopentane and stored at −80°C or fixed with Bouin's solution (Sigma, USA) and embedded with paraffin for histological studies.

Oligonucleotides

The BMSP-PMO and R-PMO peptide conjugates were synthesized and purified to >90% purity by H.M.M. (Oregon State University, Corvallis, OR, USA). The sequences of peptide B-MSP or R is

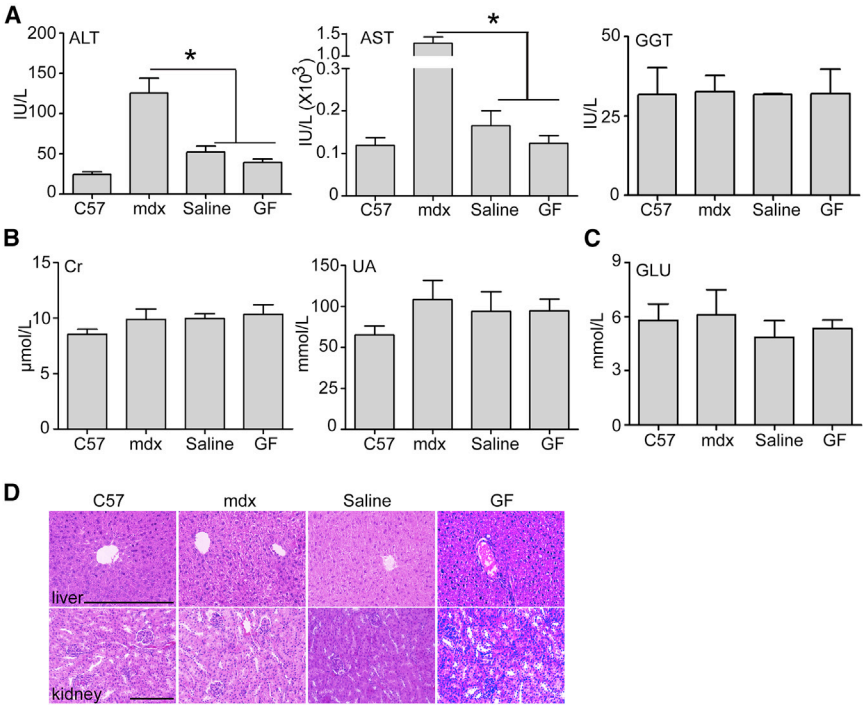

Figure 6. Measurements of Liver and Kidney Functions in Adult *mdx* Mice Treated with BMSP-PMO-GF or BMSP-PMO-S at 20 mg/kg

(A) Measurement of serum levels of liver enzymes in adult *mdx* mice treated with BMSP-PMO-GF compared to untreated age-matched *mdx* controls (n = 3, *p < 0.05). Analysis of biochemical indicators for kidney function (B) and glucose (C) in adult *mdx* mice treated with BMSP-PMO-GF or BMSP-PMO-S. Data show no difference in the level of serum creatinine (Cr), urea (UA), and glucose in *mdx* mice treated with BMSP-PMO-GF compared to untreated *mdx* and normal controls (n = 3). (D) H&E staining of liver (upper panel) and kidney (lower panel) tissues sections from treated *mdx* mice and untreated *mdx* and *C57BL6* controls (scale bar, 100 μm). Significance was determined with a two-tailed t test.

RXRRBRRXRRBRXB-ASSLNIAX or $(RXR)_4$ XB.[14,15] PMO was synthesized and purified by GeneTools (Corvallis, OR, USA). PMO (5′-GGCCAAACCTCGGCTTACCTGAAAT-3′) sequence was targeted to murine dystrophin exon 23/intron 23 boundary sites, as reported previously.[34] The PMO was conjugated to carboxyl groups at the C terminus of BMSP or R peptide using a method described elsewhere.[35]

RNA Extraction and Nested RT-PCR Analysis

Total RNA was extracted with TRIzol (Invitrogen, UK), as per the manufacturer's instructions, from BMSP-PMO-treated muscles, and 400 ng RNA template was used for 20 μL RT-PCR with OneStep RT-PCR kit (QIAGEN, UK), as described previously.[11] The primer sequences for the initial RT-PCR were exon 20 F0: 5′-CAGAATTCTGC CAATTGCTGAG-3′ and exon 26 R0: 5′-TTCTTCAGCTTTTGTGT CATCC-3′ for reverse transcription from mRNA and amplification of cDNA from exons 20 to 26. The primer sequences for the second round were exon 20 F1: 5′-CCCAGTCTACCACCCTATCAGAGC-3′ and exon 24 R1: 5′-CCTGCCTTTAAGGCTTCCTT-3′. The products were examined by electrophoresis on a 2% agarose gel.

Immunohistochemistry and Histology

A series of 8-μm sections was examined for dystrophin, DAPC, and macrophages with a series of polyclonal and monoclonal antibodies, as described elsewhere.[11] Routine H&E staining was used to examine liver and kidney morphology. For the IgG immunostaining, goat anti-mouse IgG Alex Fluor 488 secondary antibody (1:200) was used as described previously.[12] The quantification of IgG-positive areas was based on the ratio between the IgG-positive area and total area of each section with ImageJ software. Three sections per mouse and three mice were measured for quantitative analysis.

Protein Extraction and Western Blot

Protein extraction and western blot were carried out as previously described.[11] Various amounts of protein from the tibialis anterior (TA) muscle of *C57BL6* mice as a positive control and 20 or 50 μg total protein from muscles of treated or untreated *mdx* mice were used unless otherwise specified. The quantification is based on band intensity and area with ImageJ software and compared with that from TA muscles of *C57BL6* mice. Briefly, the densitometric intensity of each band including dystrophin and α-actinin was measured, and then the dystrophin values were divided by their respective α-actinin values. The dystrophin:α-actinin ratios of treated samples were normalized to the average *C57BL6* dystrophin:α-actinin ratios (from serial dilutions).

Functional Grip Strength

Treated and control mice were tested using a commercial grip strength monitor (Chatillon, UK). The procedure was performed as previously described.[11] Briefly, mice were held 2 cm from the base of the tail, allowed to grip a protruding metal triangle bar attached to the apparatus with their forepaws, and pulled gently until they released their grip. The force exerted was recorded and five sequential tests were carried out for each mouse, averaged at 30 s apart. Subsequently, the readings for force recovery were normalized by the body weight.

Clinical Biochemistry

Serum and plasma were taken from the jugular vein immediately after sacrifice with CO_2 inhalation. Analysis of serum CK, AST, ALT, GGT, Cr, urea, and CK-MB was performed by the clinical pathology laboratory (Tianjin Medical University, Metabolic Hospital, Tianjin, China).

ATP Assay

The extraction of ATP from muscles was the same as described previously.[11] Briefly, muscles were harvested and snap-frozen in liquid

nitrogen, and 10–20 mg of 4- to 6-μm-thick cryosections was collected into a 1.5-mL Eppendorf tube. 0.4 M $HClO_4$ (600 μL) was added to dissolve sections followed by vortexing for 1 min on ice. The tube was spun for 5 min at 2,000 rpm at 4°C, and the supernatant was transferred to a new tube and another 400 μL 0.4 M HClO4 was added into the precipitate, followed by centrifugation as in the previous step. Subsequently, the supernatant was spun at 4°C for 5 min at 2,000 rpm to remove debris, and it was stored for assay. CellTiter-Glo Luminescent Cell Viability Assay kit (Promega, WI, USA) was used to measure the ATP level from muscles extraction.

Masson's Trichrome Staining

Masson's trichrome staining kit (Solarbio, China) was applied for the collagen staining as described previously.[12] Briefly, a series of 8-μm sections was fixed overnight in Bouin's solution, followed by staining with the kit as per the manufacturer's instructions. The collagen-positive area was measured by ImageJ software, and 3 sections per mouse and 3 mice per group were measured. For each section, we calculated the ratio between the collagen-positive area and total area of sections.

ELISA for PMO

ELISA was used to detect the amount of PMO in muscle tissues as described previously.[12] Briefly, a DNA probe was designed with sequences complementary to PMO (synthesized by The Beijing Genomics Institute, Beijing, China) as follows: 5′-ATTTCAGGTAAGCCGAG GTTTGGCC-3′, with phosphorothioate ends in bold. The 5′ and 3′ ends of the probe were labeled with digoxigenin and biotin, respectively. Standard BMSP-PMO samples and muscle tissues (100 mg/mL) were digested with 20 mg/mL proteinase K at 55°C overnight. To avoid the interference of peptide in the detection, the digested samples were further incubated in 2.5 mg/mL trypsin at 37°C overnight.

Following PMO-probe hybridization, the avidin-biotin interaction of the hybridized probe was performed on Pierce NeutrAvidin Coated 96-well plates, Black (Thermo Fisher Scientific, MA, USA). Unhybridized probes were digested with micrococcal nuclease at 10 U/μL (Thermo Fisher Scientific, MA, USA). Then the hybridized probes were reacted with rabbit monoclonal antibody (1:1,000; Cell Signaling Technology, MA, USA) to digoxigenin, followed by detection with peroxidase-conjugated goat anti-rabbit IgG (Abcam, Cambridge, UK). Signals from the PMO-hybridized probe were detected at 450 nm with TME Substrate (Solarbio, Beijing, China) in a monochromator EnSpire Multimode plate reader (PerkinElmer, Boston, MA, USA).

Cardiac Function Measurements

Cardiac structure and function were assessed by echocardiography as described elsewhere.[36,37] Briefly, echocardiography was performed on *C57BL6*, untreated *mdx* and treated *mdx* mice in mono-dimensional mode (M-Mode) with a high-resolution transducer at a frequency of 30 MHz (VisualSonics Vevo770, Canada). Mice were held in the supine position and anesthetized by isoflurane with the shaved anterior chest wall. Warm ultrasound gel was applied to the shaved chest, and the transducer probe was placed over the left hemithorax. Parasternal and short-axis two-dimensional images of the left ventricle were acquired to determine the correct M-Mode cursor positioning. Multiple short-axis M-Mode images were acquired and the images were analyzed for left ventricle functions. Heart rate was determined from at least three consecutive RR intervals. The left ventricle M-Mode trace was used to measure EF, FS, and left ventricle mass.

Data Analysis

All data are reported as mean values ± SEM. Statistical differences between different treated groups were evaluated by SigmaStat (Systat Software, Chicago, IL, USA). Both parametric and non-parametric analyses were applied, in which the Mann-Whitney rank-sum test (Mann-Whitney U test) was used for samples on a non-normal distribution whereas a two-tailed t test was performed for samples with a normal distribution, respectively.

SUPPLEMENTAL INFORMATION

Supplemental Information can be found online at https://doi.org/10.1016/j.omtn.2019.09.012.

AUTHOR CONTRIBUTIONS

H.Y. conceived the project. G.H. and H.Y. designed the experiments, analyzed the data, and wrote the manuscript with input from all authors. G.H., B.G., C.L., H.N., J.S., and X.G. carried out the experiments. H.M.M. synthesized the peptide-PMO conjugates.

CONFLICTS OF INTEREST

The authors declare no competing interests.

ACKNOWLEDGMENTS

The authors acknowledge Dr. Yiqi Seow (Biomedical Sciences Institutes, A*STAR, Singapore) for critical review of the manuscript and Dr. Wenyan Niu (Tianjin Metabolic Disease Hospital, Tianjin Medical University, Tianjin, China) for assistance with the clinical biochemistry assays. This study was funded by the National Key R&D Program of China (grant 2017YFC1001902), the National Natural Science Foundation of China (grants 81672124 and 81802124), the Postdoctoral Science Foundation of China (grant 2017M611176), the Tianjin Municipal Science and Technology Key Project (grant 18JCQNJC79400), The Science &Technology Development Fund of Tianjin Education Commission for Higher Education (grant 2016YD10), and the Tianjin Municipal 13th five-year plan (Tianjin Medical University Talent Project).

REFERENCES

1. Nowak, K.J., and Davies, K.E. (2004). Duchenne muscular dystrophy and dystrophin: pathogenesis and opportunities for treatment. EMBO Rep. *5*, 872–876.

2. Aartsma-Rus, A., and Krieg, A.M. (2017). FDA Approves Eteplirsen for Duchenne Muscular Dystrophy: The Next Chapter in the Eteplirsen Saga. Nucleic Acid Ther. *27*, 1–3.

3. Mendell, J.R., Rodino-Klapac, L.R., Sahenk, Z., Roush, K., Bird, L., Lowes, L.P., Alfano, L., Gomez, A.M., Lewis, S., Kota, J., et al.; Eteplirsen Study Group (2013). Eteplirsen for the treatment of Duchenne muscular dystrophy. Ann. Neurol. *74*, 637–647.

4. Echigoya, Y., Lim, K.R.Q., Trieu, N., Bao, B., Miskew Nichols, B., Vila, M.C., Novak, J.S., Hara, Y., Lee, J., Touznik, A., et al. (2017). Quantitative Antisense Screening and Optimization for Exon 51 Skipping in Duchenne Muscular Dystrophy. Mol. Ther. *25*, 2561–2572.
5. McClorey, G., and Banerjee, S. (2018). Cell-Penetrating Peptides to Enhance Delivery of Oligonucleotide-Based Therapeutics. Biomedicines *6*, E51.
6. Nance, M.E., Hakim, C.H., Yang, N.N., and Duan, D. (2018). Nanotherapy for Duchenne muscular dystrophy. Wiley Interdiscip. Rev. Nanomed. Nanobiotechnol. *10*, https://doi.org/10.1002/wnan.1472.
7. Dinca, A., Chien, W.M., and Chin, M.T. (2016). Intracellular Delivery of Proteins with Cell-Penetrating Peptides for Therapeutic Uses in Human Disease. Int. J. Mol. Sci. *17*, 263.
8. Gao, X., Ran, N., Dong, X., Zuo, B., Yang, R., Zhou, Q., Moulton, H.M., Seow, Y., and Yin, H. (2018). Anchor peptide captures, targets, and loads exosomes of diverse origins for diagnostics and therapy. Sci. Transl. Med. *10*, eaat0195.
9. Kendall, G.C., Mokhonova, E.I., Moran, M., Sejbuk, N.E., Wang, D.W., Silva, O., Wang, R.T., Martinez, L., Lu, Q.L., Damoiseaux, R., et al. (2012). Dantrolene enhances antisense-mediated exon skipping in human and mouse models of Duchenne muscular dystrophy. Sci. Transl. Med. *4*, 164ra160.
10. Wang, D.W., Mokhonova, E.I., Kendall, G.C., Becerra, D., Naeini, Y.B., Cantor, R.M., Spencer, M.J., Nelson, S.F., and Miceli, M.C. (2018). Repurposing Dantrolene for Long-Term Combination Therapy to Potentiate Antisense-Mediated DMD Exon Skipping in the mdx Mouse. Mol. Ther. Nucleic Acids *11*, 180–191.
11. Han, G., Gu, B., Cao, L., Gao, X., Wang, Q., Seow, Y., Zhang, N., Wood, M.J., and Yin, H. (2016). Hexose enhances oligonucleotide delivery and exon skipping in dystrophin-deficient mdx mice. Nat. Commun. *7*, 10981.
12. Han, G., Lin, C., Ning, H., Gao, X., and Yin, H. (2018). Long-Term Morpholino Oligomers in Hexose Elicits Long-Lasting Therapeutic Improvements in mdx Mice. Mol. Ther. Nucleic Acids *12*, 478–489.
13. Yamamoto, T., Awano, H., Zhang, Z., Sakuma, M., Kitaaki, S., Matsumoto, M., Nagai, M., Sato, I., Imanishi, T., Hayashi, N., et al. (2018). Cardiac Dysfunction in Duchenne Muscular Dystrophy Is Less Frequent in Patients With Mutations in the Dystrophin Dp116 Coding Region Than in Other Regions. Circ. Genom. Precis. Med. *11*, e001782.
14. Yin, H., Moulton, H.M., Betts, C., Seow, Y., Boutilier, J., Iverson, P.L., and Wood, M.J. (2009). A fusion peptide directs enhanced systemic dystrophin exon skipping and functional restoration in dystrophin-deficient mdx mice. Hum. Mol. Genet. *18*, 4405–4414.
15. Yin, H., Moulton, H.M., Seow, Y., Boyd, C., Boutilier, J., Iverson, P., and Wood, M.J. (2008). Cell-penetrating peptide-conjugated antisense oligonucleotides restore systemic muscle and cardiac dystrophin expression and function. Hum. Mol. Genet. *17*, 3909–3918.
16. Madani, F., Lindberg, S., Langel, U., Futaki, S., and Gräslund, A. (2011). Mechanisms of cellular uptake of cell-penetrating peptides. J. Biophys. *2011*, 414729.
17. Ezzat, K., Helmfors, H., Tudoran, O., Juks, C., Lindberg, S., Padari, K., El-Andaloussi, S., Pooga, M., and Langel, U. (2012). Scavenger receptor-mediated uptake of cell-penetrating peptide nanocomplexes with oligonucleotides. FASEB J. *26*, 1172–1180.
18. Yin, H., Boisguerin, P., Moulton, H.M., Betts, C., Seow, Y., Boutilier, J., Wang, Q., Walsh, A., Lebleu, B., and Wood, M.J. (2013). Context Dependent Effects of Chimeric Peptide Morpholino Conjugates Contribute to Dystrophin Exon-skipping Efficiency. Mol. Ther. Nucleic Acids *2*, e124.
19. Aoki, Y., Nagata, T., Yokota, T., Nakamura, A., Wood, M.J., Partridge, T., and Takeda, S. (2013). Highly efficient in vivo delivery of PMO into regenerating myotubes and rescue in laminin-α2 chain-null congenital muscular dystrophy mice. Hum. Mol. Genet. *22*, 4914–4928.
20. Adamo, C.M., Dai, D.F., Percival, J.M., Minami, E., Willis, M.S., Patrucco, E., Froehner, S.C., and Beavo, J.A. (2010). Sildenafil reverses cardiac dysfunction in the mdx mouse model of Duchenne muscular dystrophy. Proc. Natl. Acad. Sci. USA *107*, 19079–19083.
21. Fayssoil, A., Renault, G., Guerchet, N., Marchiol-Fournigault, C., Fougerousse, F., and Richard, I. (2013). Cardiac characterization of mdx mice using high-resolution doppler echocardiography. J. Ultrasound Med. *32*, 757–761.
22. Stuckey, D.J., Carr, C.A., Camelliti, P., Tyler, D.J., Davies, K.E., and Clarke, K. (2012). In vivo MRI characterization of progressive cardiac dysfunction in the mdx mouse model of muscular dystrophy. PLoS ONE *7*, e28569.
23. Bendz, R., Ström, S., and Olin, C. (1980). CK-MB in serum and in heart and skeletal muscles in patients subjected to mitral valve replacement. Eur. J. Cardiol. *12*, 25–39.
24. Chapelle, J.P., el Allaf, M., Larbuisson, R., Limet, R., Lamy, M., and Heusghem, C. (1986). The value of serum CK-MB and myoglobin measurements for assessing perioperative myocardial infarction after cardiac surgery. Scand. J. Clin. Lab. Invest. *46*, 519–526.
25. Hathout, Y., Marathi, R.L., Rayavarapu, S., Zhang, A., Brown, K.J., Seol, H., Gordish-Dressman, H., Cirak, S., Bello, L., Nagaraju, K., et al. (2014). Discovery of serum protein biomarkers in the mdx mouse model and cross-species comparison to Duchenne muscular dystrophy patients. Hum. Mol. Genet. *23*, 6458–6469.
26. McMillan, H.J., Gregas, M., Darras, B.T., and Kang, P.B. (2011). Serum transaminase levels in boys with Duchenne and Becker muscular dystrophy. Pediatrics *127*, e132–e136.
27. Del Campo, A., Jaimovich, E., and Tevy, M.F. (2016). Mitochondria in the Aging Muscles of Flies and Mice: New Perspectives for Old Characters. Oxid. Med. Cell. Longev. *2016*, 9057593.
28. Zhang, H., Ryu, D., Wu, Y., Gariani, K., Wang, X., Luan, P., D'Amico, D., Ropelle, E.R., Lutolf, M.P., Aebersold, R., et al. (2016). NAD^+ repletion improves mitochondrial and stem cell function and enhances life span in mice. Science *352*, 1436–1443.
29. Wu, B., Moulton, H.M., Iversen, P.L., Jiang, J., Li, J., Li, J., Spurney, C.F., Sali, A., Guerron, A.D., Nagaraju, K., et al. (2008). Effective rescue of dystrophin improves cardiac function in dystrophin-deficient mice by a modified morpholino oligomer. Proc. Natl. Acad. Sci. USA *105*, 14814–14819.
30. Crisp, A., Yin, H., Goyenvalle, A., Betts, C., Moulton, H.M., Seow, Y., Babbs, A., Merritt, T., Saleh, A.F., Gait, M.J., et al. (2011). Diaphragm rescue alone prevents heart dysfunction in dystrophic mice. Hum. Mol. Genet. *20*, 413–421.
31. Wasala, N.B., Yue, Y., Vance, J., and Duan, D. (2017). Uniform low-level dystrophin expression in the heart partially preserved cardiac function in an aged mouse model of Duchenne cardiomyopathy. J. Mol. Cell. Cardiol. *102*, 45–52.
32. van Putten, M., van der Pijl, E.M., Hulsker, M., Verhaart, I.E., Nadarajah, V.D., van der Weerd, L., and Aartsma-Rus, A. (2014). Low dystrophin levels in heart can delay heart failure in mdx mice. J. Mol. Cell. Cardiol. *69*, 17–23.
33. Deconinck, A.E., Rafael, J.A., Skinner, J.A., Brown, S.C., Potter, A.C., Metzinger, L., Watt, D.J., Dickson, J.G., Tinsley, J.M., and Davies, K.E. (1997). Utrophin-dystrophin-deficient mice as a model for Duchenne muscular dystrophy. Cell *90*, 717–727.
34. Harding, P.L., Fall, A.M., Honeyman, K., Fletcher, S., and Wilton, S.D. (2007). The influence of antisense oligonucleotide length on dystrophin exon skipping. Mol. Ther. *15*, 157–166.
35. Moulton, H.M., Nelson, M.H., Hatlevig, S.A., Reddy, M.T., and Iversen, P.L. (2004). Cellular uptake of antisense morpholino oligomers conjugated to arginine-rich peptides. Bioconjug. Chem. *15*, 290–299.
36. Spurney, C.F., Gordish-Dressman, H., Guerron, A.D., Sali, A., Pandey, G.S., Rawat, R., Van Der Meulen, J.H., Cha, H.J., Pistilli, E.E., Partridge, T.A., et al. (2009). Preclinical drug trials in the mdx mouse: assessment of reliable and sensitive outcome measures. Muscle Nerve *39*, 591–602.
37. Chaudhari, M.R., Fallavollita, J.A., and Farkas, G.A. (2016). The Effects of Experimental Sleep Apnea on Cardiac and Respiratory Functions in 6 and 18 Month Old Dystrophic (mdx) Mice. PLoS ONE *11*, e0147640.